Learning Nonlinear Couplings in Network of Agents From a Single Sample Trajectory

Arash Amini, Qiyu Sun, and Nader Motee, *Senior Member, IEEE*

***Abstract*—In this article, we study a class of stochastic nonlinear dynamical networks governed by coupling functions, showing that under certain assumptions, these networks can produce geometrically ergodic trajectories. Our findings suggest that a wide range of coupling functions can be effectively learned from just one sample trajectory in the network. This approach is practical, as it often aligns with the preference in many applications to conduct a single, extended experiment rather than repeating the same experiment under different initial conditions. Drawing on concentration inequalities for geometrically ergodic Markov chains, we present several results regarding the empirical estimator's convergence to the actual coupling function, substantiated by extensive simulations.**

***Index Terms*—Machine learning, nonlinear couplings, statistical learning, stochastic dynamical networks.**

I. Introduction

INTERACTION among members of a community plays a crucial role in the emergence of holistic behaviors in various natural and engineering systems ranging from interacting atoms to form complex molecules, herd of bison, social networks, the platoon of self-driving cars, interconnected power networks, evolution, and reform mechanisms in financial markets. These interactions may occur via swarm dynamics, such as flow interactions within a school of fish [1], or through shared control objectives, such as robot navigation based on potential functions [2]. There have been several fundamental studies to mathematically explain interactions in some of these systems [3], [4], [5], [6], where the standard approach is to leverage the underlying logic and physics of such systems and obtain a proper coupling function, by trial and error, in order to replicate collective dynamic behavior of these systems using computer simulations.

The recent advancements in statistical learning theories [7], [8] combined with the dramatic growth of computational power have provided a solid foundation to learn large-scale dynamics from extensive sensory data in an end-to-end manner. This breakthrough resulted in intensive research on learning dynamical systems [9], [10], [11], [12], [13]. A major challenge in learning dynamical networks is the curse of dimensionality, i.e., as the number of agents increases, the computation becomes very expensive and the learning accuracy deteriorates rapidly by the network size. It is worth noting that significant reductions in computational costs can be achieved if the underlying dynamics to be learned demonstrate specific structures. For instance, in some applications, the dynamics of the entire network can be inferred by learning a common coupling function among the agents [14], [15].

The class of networks with gradient-type interaction laws is investigated in [14], where it is shown that increasing the number of agents will improve the approximation accuracy. A class of homogeneous and heterogeneous networks is considered in [15] and [16], where the authors show that one can learn the coupling functions using multiple sample trajectories with guaranteed convergence. The closest work in spirit to this article is [17], where the authors prove that one can learn the coupling functions with only one trajectory in the presence of Gaussian noise if the interaction law is of gradient type and the dynamics of the resulting network is *linear*. In this article, we address the problem of learning a *general* class of coupling functions in the presence of bounded stochastic noise using only one single sample trajectory.

The idea of learning dynamical systems using a single sample trajectory [18] is practically plausible as in numerous applications, it is more feasible and cost-effective to collect samples from an ongoing experiment rather than repeating the same experiment multiple times under different initial conditions. Few articles aim to address the problem of learning nonlinear dynamics from single sample trajectory [19], [20], and those existing works focus on learning individual nonlinear systems [21], [22], whereas a key contribution of our work is presenting an approach that can handle learning the couplings in a large-scale network of interconnected nonlinear subsystems. This allows us to address the curse of dimensionality that arises when applying machine learning techniques to complex networked dynamical systems. By exploiting the specific structure of couplings in the network, we proved that the learning couplings from a single sample trajectory converge independently from the number of agents in the networks, overcoming the limitations of general frameworks.

Our main distinct contributions with respect to the existing literature are twofold. First, we prove that a class of stochastic dynamical networks can generate geometrically ergodic trajectories under some technical assumptions, i.e., the joint evolution

Received 19 November 2023; revised 29 November 2023 and 12 April 2024; accepted 23 June 2024. Date of publication 17 September 2024; date of current version 20 March 2025. This work was supported by ONR under Grant N00014-23-1-2779. Recommended by Associate Editor K. Savla. *(Corresponding author: Arash Amini.)*

Arash Amini and Nader Motee are with the Department of Mechanical Engineering and Mechanics, Lehigh University, Bethlehem, PA 18015 USA (e-mail: a.amini@lehigh.edu; motee@lehigh.edu).

Qiyu Sun is with the Department of Mathematics, University of Central Florida, Orlando, FL 32816 USA (e-mail: qiyu.sun@ucf.edu).

Digital Object Identifier 10.1109/TCNS.2024.3462850

probability distribution of trajectories will converge geometrically fast to an invariant stationary distribution; see Theorem 1. This development is necessary to ensure that collecting new sample points along the same trajectory will contain valuable information for learning purposes. Building upon this result, in our second main contribution, we prove that for such geometrically ergodic stochastic dynamical networks, one can learn a class of nonlinear coupling functions using only one single sample trajectory over a convex and compact hypothesis space that satisfies the coercivity condition; see Theorem 3. We then show that as the length of the sample trajectory increases, the learning accuracy enhances accordingly up to its limit with high confidence levels. In this case, the approximation error, i.e., the distance between the true coupling function and its approximation, tends to be the distance between the true coupling function and the space of hypothesis functions. If the actual coupling function lies inside the space of the hypothesis functions, then the approximation error will tend to zero; see Theorem 3. Finally, when the class of bounded Lipschitz functions is adopted as the hypothesis space and the true coupling function belongs to this space, we provide an upper bound for the expected value of the learning error and quantify the convergence rate for the error functional in terms of the length of the sample trajectory; see Theorem 4.

Mathematical Notations: We employ the operator; to concatenate two column vectors $x, y \in \mathbb{R}^d$ to obtain column vector $[x; y] \in \mathbb{R}^{2d}$. The symbol $\otimes$ represents the Kronecker product, and $\mathbb{1} = [1, \dots, 1]^{\mathsf{T}} \in \mathbb{R}^n$ is the vector of all ones.

II. Problem Statement

Let us consider a class of stochastic interconnected dynamical networks whose dynamics are governed by

$$x_{t+1}^i = x_t^i + h\sum_{j=1}^{n} k_{ij}\phi\left(\|x_t^j - x_t^i\|\right)\left(x_t^j - x_t^i\right) + hw_t^i \quad (1)$$

with initial condition x_0^i, for all $t \in \mathbb{Z}_+$ and $i \in \mathcal{V} := \{1, \dots, n\}$, where h is the sampling time, $x_t^i \in \mathbb{R}^d$ is the state of agent i at time instant ht, and $w_t^i \in \mathbb{R}^d$ represents the stochastic effect of environment on the dynamics of agent i at time ht, which is assumed to be independent of x_t^i for all $t \geq 0$. The interaction between agents i and j is modeled by a coupling function $\phi : \mathbb{R} \to \mathbb{R}$ and their coupling strength by coefficients $k_{ij} \geq 0$. Agents i and j are coupled iff $k_{ij} \neq 0$. By defining the vector of state variables $x_t = [x_t^1; \dots; x_t^n]$ and noise input $w_t = [w_t^1; \dots; w_t^n]$, the overall dynamics of the network can be rewritten in a compact form

$$x_{t+1} = (I - hL_{x_t})x_t + hw_t \quad (2)$$

where the (i, j)th entry of the state-dependent Laplacian matrix of the underlying graph of the network L_{x_t} is defined as

$$(L_{x_t})_{ij} = \begin{cases} -k_{ij}\phi(r_t^{ij})I_d, & \text{if } j \neq i \\ \sum_{m\in\mathcal{V}\setminus i} k_{im}\phi(r_t^{im})I_d, & \text{if } j = i \end{cases} \quad (3)$$

where the relative state of agent j with respect to agent i is defined by $\mathrm{r}_t^{ij} = x_t^j - x_t^i$ with $r_t^{ij} = \|\mathrm{r}_t^{ij}\|$. We define the maximum of weights over the network by $K := \max\{k_{ij} \,|\, 1 \leq i, j \leq n\}$. Throughout this article, we assume that the entries of the initial condition x_0 of network (2) are bounded random variables and $\|x_0\| \leq R_0$ holds almost surely for some constant $R_0 > 0$. Moreover, it is assumed that each entries of w_t are bounded independent identically distributed (i.i.d.) random variable with

$$\mathbb{E}[w_t] = 0,\ \mathbb{E}\left[w_t w_t^{\mathsf{T}}\right] = I \otimes \Sigma,\ \text{and}\ \|w_t\| \leq \omega \quad (4)$$

for all $t \in \mathbb{Z}_+$, holds almost surely for some constant $\omega > 0$, which satisfies $\sigma^2 := n\mathrm{Tr}(\Sigma) \leq \omega^2$.

We rewrite (2) as

$$x_{t+1} = x_t + hF_\phi(x_t) + hw_t \quad (5)$$

where

$$\left(F_\phi(x_t)\right)_i = -\sum_{j=1}^{n} k_{ij}\phi(r_t^{ij})\mathrm{r}_t^{ij}. \quad (6)$$

For a given coupling function $\psi : \mathbb{R} \longmapsto \mathbb{R}$, we define

$$\mathcal{E}_{x_t}(\psi) := \frac{1}{N_e}\left\|\frac{x_{t+1} - x_t}{h} - F_\psi(x_t)\right\|^2 = \frac{1}{N_e}\left\|F_{\psi-\phi} - w_t\right\|^2 \quad (7)$$

where N_e is the number of edges in the underlying network. Let $\mathcal{H}$ be a class of candidate functions that satisfies Assumption 4. We formulate the empirical error for a given candidate function $\psi \in \mathcal{H}$ by

$$\mathcal{E}_T(\psi) := \frac{1}{TN_e}\sum_{t=1}^{T}\left\|\frac{x_{t+1} - x_t}{h} - F_\psi(x_t)\right\|^2 \quad (8)$$

where T stands for the length of the sample trajectory. Our goal is to learn coupling function ϕ by solving the optimization problem

$$\hat{\phi}_T = \arg\min_{\psi\in\mathcal{H}} \mathcal{E}_T(\psi). \quad (9)$$

The *problem* is to learn the coupling function $\phi : \mathbb{R} \to \mathbb{R}$ using a single, long enough, sample trajectory $x_0, x_1, \dots, x_T$ of the dynamical network (2) by solving (9) and show that by increasing the length of the sampled trajectory T, the distance between $\hat{\phi}_T$, the optimal solution of (9), and the true coupling function, ϕ, known as the approximation error, will tend to the distance of ϕ from $\mathcal{H}$. If $\phi \in \mathcal{H}$, then the approximation error will go to zero.

III. Properties of the Dynamical Network

To guarantee certain properties for a dynamical network (1), the true coupling function and the underlying graph of the network should satisfy a few conditions.

Assumption 1: The coupling function ϕ is positive, continuous on $[0, \infty)$, differentiable at zero, and upper bounded by $S_0 > 0$.

The underlying weighted graph of network (2) with Laplacian matrix L_x is denoted by $\mathcal{G}_x$. Since the coupling function ϕ is positive, there exists an edge between agents i and j in $\mathcal{G}_x$ if and only if $k_{ij} > 0$. Thus, one only needs to evaluate the properties of graph $\mathcal{G}_0$, i.e., $\mathcal{G}_x$ at $x = 0$.

Assumption 2: The graph $\mathcal{G}_0$ is undirected, simple, and connected.

We emphasize that the graph $\mathcal{G}_0$ is an undirected graph with no self-coupling, which implies $k_{ij} = k_{ji}$ for all $(i, j) \in \mathcal{V} \times \mathcal{V}$ and $k_{ii} = 0$ for all $i \in V$. The eigenspace of the Laplacian L_x associated with the eigenvalue zero is the diagonal subspace

$$\Delta = \left\{ [u; \dots; u] \middle| u \in \mathbb{R}^d \right\}. \tag{10}$$

Every vector $x \in \mathbb{R}^{dn}$ can be decomposed as $x = \bar{x} + x_\perp$, where

$$\bar{x} := \frac{1}{n} \mathbb{1} \otimes \left(\sum_{i=1}^{n} x^i \right)$$

is its projection onto Δ, and $x_\perp$ is its projection onto $\Delta^\perp$, the orthogonal complement of Δ in $\mathbb{R}^{dn}$. We can accordingly decompose the dynamics of network (2) as

$$x_{t+1,\perp} = (I - hL_{(x_{t,\perp})})x_{t,\perp} + hw_{t,\perp} \tag{11}$$

and

$$\bar{x}_{t+1} = \bar{x}_t + h\bar{w}_t. \tag{12}$$

The projection of w_t onto $\Delta^\perp$ is given by $w_{t,\perp} := w_t - \bar{w}_t$, which has expected values 0 and $\mathbb{E}[w_{t,\perp} w_{t,\perp}^\mathsf{T}] = M_n \otimes \Sigma$, where $M_n = I - \frac{1}{n}\mathbb{1}\mathbb{1}^\mathsf{T}$ is the centering matrix. The dynamical system (12) is independent of the coupling function ϕ, which implies that its trajectories do not contain any useful information to learn the coupling function ϕ. Therefore, only the orthogonal part of the trajectories is informative. For simplicity of our notations, we rewrite (11) as

$$x_{t+1} = (I - hL_{x_t})x_t + hw_t \tag{13}$$

where $x_t \in \Delta^\perp$, and update $\mathbb{E}[w_t w_t^\mathsf{T}] = M_n \otimes \Sigma$. The eigenvalues of $I - hL_{x_t}$ are contained in $[1 - h\lambda_{\max}(L_{x_t}), 1 - h\lambda_2(L_{x_t})]$, where $\lambda_2(L_{x_t})$ and $\lambda_{\max}(L_{x_t})$ are the smallest nonzero and the largest eigenvalue of L_{x_t}, respectively. We remark that, as x_t is orthogonal to $\mathbb{1}$, the eigenspace associated with eigenvalue one of L_{x_t}, which is generated by $\mathbb{1}$, does not affect the informative part of the state $x_t \in \Delta^\perp$.

Assumption 3: The dynamics of (13) is uniformly contractive on $\Delta^\perp$, or equivalently, the maximum Laplacian eigenvalue satisfies $\lambda_{\max}(L_{x_t}) < \frac{2}{h}$ along all trajectories of the system.

We emphasize that (1) discretizes a continuous time system, and Assumption 3 on the uniform contractivity of the dynamics of (13) is satisfied if the step size h is chosen to be sufficiently small. In fact, the spectral radius of the Laplacian satisfies

$$\zeta := \sup_{t \geq 0} \max \left\{ |1 - h\lambda_2(L_{x_t})|, |1 - h\lambda_{\max}(L_{x_t})| \right\} < 1. \tag{14}$$

Example 1: To better understand the above-mentioned assumption, one can verify that the dynamics of network (3) will satisfy Assumption 3 if $\mathcal{G}_x$ is a complete graph and $h < \frac{1}{nKS_0}$ or $\mathcal{G}_x$ is a path graph and $h < \frac{1}{2KS_0}$, where S_0 is defined in Assumption 1 and $K = \max\{k_{ij} \mid 1 \leq i, j \leq n\}$. In general, system (13) is uniformly contractive on $\Delta^\perp$ if $h \leq \tilde{K}S_0)^{-1}$, where $\tilde{K} = \max_{1 \leq i \leq n} \sum_{j=1}^{n} k_{ij}$.

Proposition 1: Suppose that the dynamical network (13), which is considered over $\Delta^\perp$, satisfies Assumption 3, the initial is chosen randomly from a distribution bounded by R_0, and disturbance w_t satisfies (4) for every $t \geq 0$. Then

$$r_t^{ij} \leq 2\left(R_0 + \frac{h\omega}{1 - \zeta} \right) \tag{15}$$

for every $1 \leq i, j \leq n$, and $t \geq 0$, holds almost surely.

The result of this proposition asserts that the relative positions of agents in the presence of bounded noise will remain bounded. In fact, it can be shown that the distance between every pair of agents is bounded by

$$R := 2\left(R_0 + \frac{h\omega}{1 - \zeta} \right). \tag{16}$$

IV. Geometric Ergodicity of the Network

Following the problem statement in Section II, our goal is to learn the coupling function from a single sample trajectory. In order to ensure that the empirical estimator converges to the expected estimator as the number of samples are increased, we prove that the Markov chain (5), under some technical assumptions, is geometrically ergodic [23], [24]. Let us consider the stochastic process

$$x_{t+1} = G(x_t, w_t) \tag{17}$$

that generates a Markov chain $\{x_t\}_{t \geq 0}$ in $\mathcal{X} \subset \mathbb{R}^{nd}$, where $w_t \in \mathbb{R}^{nd}$ are i.i.d. random variables with bounded distribution. The tth step transition probability of this Markov chain is defined by

$$\mathbb{P}^t(x, A) = \mathbb{P}(x_t \in A | \, x_0 = x) \tag{18}$$

for $x \in \mathcal{X}$ and $A \in \mathbb{B}$, in which $\mathbb{B}$ is the set of all Borel sets [25].

Definition 1: The stochastic process $\{x_t\}_{t \geq 0}$ generated by (17) is geometrically ergodic if there exists a probability measure π on $(\mathbb{R}, \mathbb{B})$, a number $0 < \rho < 1$, and a π-integrable nonnegative measurable function $h : \mathbb{R}^d \to \mathbb{R}$ such that

$$\|\mathbb{P}^t(x, \cdot) - \pi(\cdot)\|_{TV} \leq \rho^t h(x) \tag{19}$$

where $\|\mathbb{P}^t(x, \cdot) - \pi(\cdot)\|_{TV} = \sup_{A \in \mathbb{B}} \left| \mathbb{P}^t(x, A) - \pi(A) \right|$ is the total variation norm [23], [24].

This definition implies that the joint probability distribution of a geometrically ergodic Markov chain converges exponentially to a stationary probability distribution π [24].

Theorem 1: Suppose that dynamical network (13) satisfies Assumptions 1–3. Then, the stochastic process $\{x_t\}_{t \geq 0}$ in $\Delta^\perp$ generated by (13) is geometrically ergodic.

Theorem 1 states that the Markov chain evolving according to (13) is geometrically ergodic, which implies that there exists an invariant probability measure π independent of the initial condition that satisfies (19). We define the empirical probability distribution $\rho_T : [0, R] \to \mathbb{R}_+$ for the network (13) by

$$\rho_T(r) := \frac{1}{N_e T} \sum_{t=0}^{T-1} \sum_{i=1}^{n} \sum_{j \in \mathcal{N}_i} \delta_{r_t^{ij}}(r) \tag{20}$$

where $\mathcal{N}_i$ is the set of all neighboring agents of agent i in graph $\mathcal{G}_0$ and

$$\delta_{r_t^{ij}}(r) = \begin{cases} 0, & \text{if } r \neq r_t^{ij} \\ 1, & \text{if } r = r_t^{ij}. \end{cases}$$

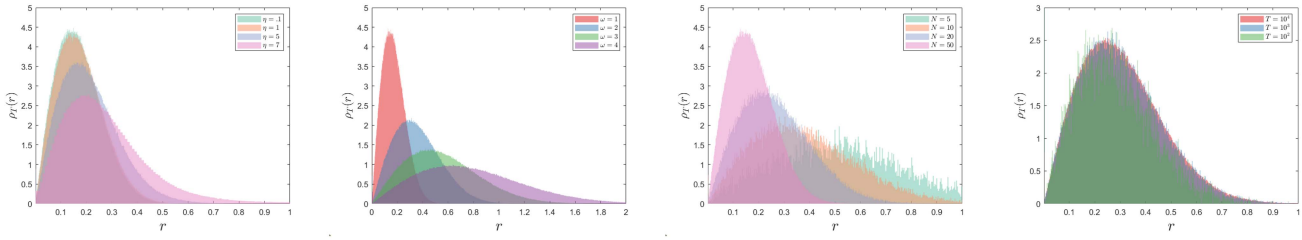

(a) (b) (c) (d)

Fig. 1. Empirical probability distribution, ρ_T, for different scenarios discussed in Example 2. (a) Coupling strength. (b) Noise amplitude. (c) Number of agents. (d) Sampling length.

By the law of large numbers (see [26, Th. 1] and [27]), it follows that:

$$\rho(r) := \lim_{T\to\infty} \rho_T(r) = \frac{1}{N_e} \sum_{i=1}^{n} \sum_{j\in\mathcal{N}_i} \mathbb{E}_\pi \left[\delta_{r_t^{ij}}(r)\right] \tag{21}$$

and

$$\lim_{T\to\infty} \frac{1}{T} \sum_{t=0}^{T-1} \|F_\psi(x_t)\|^2 = \mathbb{E}_\pi \left[\|F_\psi(x)\|^2\right] \tag{22}$$

where π is the invariant probability measure from Theorem 1.

For a given $r \in [0, R]$, the quantity $\rho(r)$ measures the fraction of neighbors whose relative distances are equal to r. Thus, for a given interval $J \subset [0,\ R]$, one can utilize $\rho(J)$ to measure how spread the samples are over $[0, R]$: the larger the value of $\rho(J)$ correspond to more distinct and informative samples.

One can assume that the number of agents and the class of candidate functions are available in most applications. Therefore, the length T of the sample trajectory controls how closely the empirical probability distribution ρ_T approximates the true stationary distribution ρ, as illustrated in Example 2.

Example 2: Let us consider the swarm dynamics (1) with $d = 2$, in which $\mathcal{G}_0$ is a complete graph, and the coupling function is

$$\phi(r) = \Gamma(1 + r^2)^{-\eta}. \tag{23}$$

This is widely known as the Cucker–Smale [4] coupling function. Fig. 1 illustrates the effect of noise amplitude ω, length of sampling T, coupling strength η, and the number of agents N on the empirical probability distribution ρ_T. Each subplot in Fig. 1 depicts the empirical measure of the probability distribution ρ_T by setting $\Gamma = 0.4$, $T = 10^4$, $\eta = 1$, $\omega = 1$, and $n = 50$ as the fixed parameters. As it is shown in Fig. 1(a), by increasing η, the coupling strength weakens, which results in a network of agents whose relative distances are more scattered. When the noise amplitude is increased, inequality (15) implies that the relative distances may experience larger fluctuations. Fig. 1(b) shows how the probability distribution ρ_T starts to flatten and spread along the axis as the noise amplitude increases. According to [28, Th. 2], if the network is ergodic, then ρ_T converges to ρ as $T \to \infty$, which is shown in Fig. 1(d).

V. Convergence of Learning

The geometric ergodicity property of the network is necessary to define the steady-state empirical probability distribution $\rho : [0, R] \to \mathbb{R}_+$, which in turn allows us to define a Hilbert space. Let us consider the space of functions $L^{2,*}_{\rho_T}([0, R])$ as the weighted Hilbert space of measurable functions with respect to $\rho_T : [0, R] \to \mathbb{R}_+$ that is endowed by

$$\|\psi\|_{L^{2,*}_{\rho_T}([0,R])} := \left(\int_0^R |\psi(r)r|^2 \rho_T(dr)\right)^{1/2} \tag{24}$$

for all $T \geq 1$. For clarity, we simply use the notation $L^{2,*}_{\rho_T}$. Using (6), one gets

$$\mathbb{E}_\pi[\|F_\psi(x)\|^2] \leq N_e K^2 \|\psi\|^2_{L^{2,*}_\rho} \tag{25}$$

where $K = \max\{k_{ij} \mid 1 \leq i, j \leq N\}$. The geometric ergodicity property of the network enables us to apply the law of large numbers to the empirical error functional and show that its expectation exists, which is defined by

$$\begin{aligned}\mathcal{E}(\psi) &:= \lim_{T\to\infty} \frac{1}{T} \sum_{t=1}^{T} \mathcal{E}_{x_t}(\psi) \\ &= \frac{1}{N_e} \left(\mathbb{E}_\pi \left[\|F_{\psi-\phi}(x)\|^2\right] + \sigma^2\right) \quad \forall \psi \in \mathcal{H}.\end{aligned} \tag{26}$$

Suppose that $\hat{\phi}$ is the estimator of the expected error functional over the hypothesis space $\mathcal{H}$, i.e.,

$$\hat{\phi} := \arg\min_{\psi\in\mathcal{H}} \mathcal{E}(\psi). \tag{27}$$

We investigate the convergence of the empirical estimator $\hat{\phi}_T$ to the true coupling function ϕ. When $\phi \in \mathcal{H}$, it can be shown that $\hat{\phi} = \phi$. For a given parameter $\delta \in (0, 1)$, our goal is to quantify the minimum trajectory length T to ensure that

$$\|\hat{\phi}_T - \hat{\phi}\|_{L^{2,*}_{\rho_T}} \leq \epsilon$$

holds with probability $1 - \delta$. First, in Section V-A, it is shown that if the hypothesis space is compact, the error of the empirical estimator converges to the error of the expected estimator. Then, in Section V-B, it is proven that if in addition to compactness the hypothesis space satisfies the convexity and coercivity conditions, then the expected estimator is also unique.

Assumption 4: The hypothesis space $\mathcal{H}$ is a bounded subset of $L^\infty([0, R])$, i.e.,

$$S_\mathcal{H} := \sup_{\psi\in\mathcal{H}} \|\psi\|_{L^\infty([0,R])} < \infty \tag{28}$$

and $S_\mathcal{H} \geq S_0$, where S_0 is the upper bound for the original coupling function ϕ.

All functions $\psi \in \mathcal{H}$ have domain $[0, R]$. To improve the tractability of our theoretical results, we simply use the notation $\|\psi\|_\infty$ instead of $\|\psi\|_{L^\infty([0,R])}$.

Remark 1: Using Assumption 4 and (24), one can show that

$$\|\psi\|_{L^{2,*}_{\rho_T}} \leq R\|\psi\|_\infty < \infty \tag{29}$$

for every $\psi \in \mathcal{H}$, which reveals a relationship between the two norms.

In the rest of this section, we present the core results regarding the convergence of the coupling function from a single sample trajectory to the original coupling. To prove Theorem 2, we employ the standard statistical learning techniques. We emphasize that in the general nonlinear learning framework [18], [20], the convergence of error functional simultaneously guarantees the convergence of the estimator to the original function. It is imperative to incorporate additional assumptions in our case to ensure such guarantees. In the later part of this section, we will discuss the necessary conditions for the estimator to be a unique estimator and provide proof for its convergence while also estimating the corresponding rates.

A. Error Convergence

Suppose the hypothesis space $\mathcal{H}$ is a compact subset of $L^\infty([0, R])$ and the expected estimator lies in $\mathcal{H}$. We show that using these minimal assumptions, one can only prove that $\mathcal{E}(\hat{\phi}_T)$ will converge to $\mathcal{E}(\hat{\phi})$ with the desired confidence if the sampled trajectory is long enough. For two given candidate functions $\psi_1, \psi_2 \in \mathcal{H}$, we show that the difference of the corresponding empirical errors of ψ_1 and ψ_2 is always bounded by the $L^{2,*}_{\rho_T}$ distance of the two functions.

Lemma 1: For every $\psi_1, \psi_2 \in \mathcal{H}$

$$|\mathcal{E}_T(\psi_1) - \mathcal{E}_T(\psi_2)| \leq 2K^2RS\|\psi_1 - \psi_2\|_{L^{2,*}_{\rho_T}} \tag{30}$$

$$|\mathcal{E}(\psi_1) - \mathcal{E}(\psi_2)| \leq 2K^2RS\|\psi_1 - \psi_2\|_{L^{2,*}_{\rho}} \tag{31}$$

hold almost surely, where $S := S_{\mathcal{H}} + \|\phi\|_\infty + \omega/R$.

For every $T \geq 1$ and $\psi \in \mathcal{H}$, let us define functional

$$L_T(\psi) := \mathcal{E}(\psi) - \mathcal{E}_T(\psi).$$

Then, for every $\psi_1, \psi_2 \in \mathcal{H}$, it follows that:

$$\begin{aligned} |L_T(\psi_1) - L_T(\psi_2)| &\leq 4K^2R^2S\|\psi_1 - \psi_2\|_\infty \\ &\leq 8K^2R^2S^2 \end{aligned} \tag{32}$$

holds almost surely, where (32) is a direct consequence of Lemma 1. Using (7), we define function $g_\psi : \mathbb{R}^{dn} \to \mathbb{R}$ by

$$g_\psi(x_t) := \mathcal{E}_{x_t}(\psi) - \mathcal{E}(\psi) \tag{33}$$

for all $\psi \in \mathcal{H}$, whose asymptotic variance is given by

$$\sigma^2_{\mathcal{M}}(\psi) = \mathrm{Var}_\pi g_\psi(x_0) + 2\sum_{i=1}^{\infty} \mathrm{Cov}_\pi \left[g_\psi(x_0), g_\psi(x_i)\right]. \tag{34}$$

where $g_\psi(x_t)$ is defined by

$$g_\psi(x_t) := \mathcal{E}_{x_t}(\psi) - \mathcal{E}(\psi) \tag{35}$$

for all $\psi \in \mathcal{H}$. In the next theorem, we prove that when the hypothesis space $\mathcal{H}$ is compact and the expected estimator $\hat{\phi}$ lies in it, then the empirical error converges to the expected error as length of the sampled trajectory, i.e., T, tends to infinity.

Theorem 2: Suppose that $\mathcal{H}$ is a compact subset of $L^\infty([0, R])$ and $\hat{\phi} \in \mathcal{H}$. Then, for every $\epsilon > 0$, we have

$$\begin{aligned} &\mathbb{P}\left\{\left|\mathcal{E}(\hat{\phi}_T) - \mathcal{E}(\hat{\phi})\right| \leq \epsilon\right\} \geq \\ &1 - C\,\mathcal{N}\left(\mathcal{H}, \frac{\epsilon}{16K^2R^2S}\right) e^{\left(\frac{-\epsilon^2 T}{512\sigma^2_{\mathcal{H}} + 32\tau\epsilon 8K^2R^2S^2\log(T)}\right)} \end{aligned} \tag{36}$$

where C and τ are constants with respect to ergodicity rate of (13), $\mathcal{N}(\mathcal{H}, l)$ is the minimum number of balls with diameter $l > 0$ required to cover $\mathcal{H}$ with respect to the L^∞ norm, and $\sigma^2_{\mathcal{H}}$ is the supremum of the asymptotic variances of random variables $g_\psi(x_t)$, i.e.,

$$\sigma^2_{\mathcal{H}} = \sup_{\psi \in \mathcal{H}} \sigma^2_{\mathcal{M}}(\psi).$$

Theorem 2 demonstrates that if the hypothesis space $\mathcal{H}_f$ is a compact subset of $L^\infty([0, R])$ and the expected estimator $\hat{\phi}$ is an element of $\mathcal{H}_f$, then the difference in error between the empirical and expected estimators can be made arbitrarily small with high probability, provided that the sample trajectory length is sufficiently large. To show that asymptotic variance $\sigma_{\mathcal{H}}$ is bounded, we leverage the fact that the network is the geometric ergodicity and the second moment of an error functional is bounded [29], [30].

B. Convergence of Empirical Estimator

For $\phi \in \mathcal{H}$, we obtain from (25) that

$$\mathbb{E}\left[\|F_{\psi-\phi}\|^2\right] \leq N_e K^2 \|\psi - \phi\|^2_{L^{2,*}_\rho}.$$

If the above inequality becomes an equality, the convexity of the hypothesis space is sufficient to prove the existence of a unique minimizer for (9) [8]. In our case, however, the convexity of $\mathcal{H}$ will not be sufficient and one has to further assume other properties to guarantee that the expected estimator is unique and lies in $\mathcal{H}$. The next assumption will allow us to ensure the learnability of our problem.

Assumption 5: The hypothesis space $\mathcal{H}$ is a compact and convex set of functions on $\mathbb{R}_+$, which satisfy the coercivity condition

$$c_{\mathcal{H}} := \frac{1}{N_e} \inf_{\psi \in \mathcal{H}\setminus\{0\}} \left\{\frac{\mathbb{E}_\pi\left[\|F_\psi(x)\|^2\right]}{\|\psi\|^2_{L^{2,*}_\rho}}\right\} > 0. \tag{37}$$

If $\psi - \phi \in \mathcal{H}$, then inequality

$$c_{\mathcal{H}}\|\psi - \phi\|^2_{L^{2,*}_\rho} \leq \mathcal{E}(\psi) - \mathcal{E}(\phi) \tag{38}$$

is a direct consequence of Assumption 5. Furthermore, one can show that

$$c_{\mathcal{H}}\|\psi - \hat{\phi}\|^2_{L^{2,*}_\rho} \leq \mathcal{E}(\psi) - \mathcal{E}(\hat{\phi}). \tag{39}$$

Thus, $\hat{\phi}$ is the unique minimizer of $\mathcal{E}$ over $\mathcal{H}$.

Theorem 3: Suppose that $\mathcal{H}$ is a compact, convex, and coercive subset of the $L^\infty([0,R])$. Then, the error bound

$$\|\hat{\phi}_T-\phi\|^2_{L^{2,*}_\rho}\leq 4\left(1+\frac{K}{c_{\mathcal{H}}}\right)\inf_{\psi\in\mathcal{H}}\|\psi-\phi\|^2_{L^{2,*}_\rho}+\frac{2\epsilon}{c_{\mathcal{H}}} \tag{40}$$

holds with probability at least $1-\delta$, for all $\epsilon>0$ and $\delta\in(0,1)$, provided that the length of the sampled trajectory T satisfies

$$C\,\mathcal{N}\left(\mathcal{H},\frac{\epsilon}{24K^2R^2S}\right)\leq \delta\exp\left\{\frac{T\epsilon}{96K^2S^2R^2\left(\frac{128c_{\mathcal{M}}K^2}{c_{\mathcal{H}}}+\tau\log(T)\right)}\right\} \tag{41}$$

where τ, C, and $c_{\mathcal{M}}$ are positive constants with respect to ergodicity rate of the network (13).

The result of Theorem 3 asserts that one can learn a coupling function with an arbitrary precision with probability $1-\delta$ if the trajectory length T is long enough.

Remark 2: If the true coupling function $\phi\in\mathcal{H}$, then for all $T\geq 1$, the error bound

$$\|\hat{\phi}_T-\phi\|^2_{L^{2,*}_\rho}\leq\frac{2\epsilon}{c_{\mathcal{H}}}$$

holds with probability at least $1-\delta$, where δ satisfies (41). The convergence rate of the empirical estimator to the true coupling function can be controlled by coercivity constant $c_{\mathcal{H}}$.

Remark 3: The bias term in (40) solely depends on the choice of the hypothesis space, which emphasizes that the coupling functions can be learned as far as the hypothesis spaces allow.

Let us define the set of functions $\mathcal{K}_{R,S}\in L^\infty([0,R])$ by

$$\mathcal{K}_{R,S}:=\left\{\psi\in\mathrm{Lip}_c([0,R])\;\middle|\;\|\psi\|_\infty+\mathrm{Lip}(\psi)\leq S\right\} \tag{42}$$

where $\mathrm{Lip}_c([0,R])$ is the class of Lipschitz functions with compact support over $[0,R]$, and c is the Lipschitz constant of ψ over the interval $[0,R]$. We finish this section by approximating the rate of convergence of the empirical estimator when $\mathcal{H}=\mathcal{K}_{R,S}$ and $\phi\in\mathcal{H}$.

Theorem 4: Suppose that $\hat{\phi}_T$ is the minimizer of the empirical error functional (8) over hypothesis space $\mathcal{H}=\mathcal{K}_{R,S}$ and $\phi\in\mathcal{K}_{R,S}$. Then, there exists a $0\leq\gamma$ such that

$$\mathbb{E}_\pi\left[\|\hat{\phi}_T-\phi\|_{L^{2,*}_\rho}\right]\leq\gamma\sqrt[4]{\frac{128c_{\mathcal{M}}K^2+\tau c_{\mathcal{H}}\log(T)}{Tc^2_{\mathcal{H}}}} \tag{43}$$

where γ is a function of R, S, and K.

Theorem 4 shows the convergence rate of the empirical estimator to the true coupling function using one single sample trajectory depending on both coercivity constant and the covariance of the noise. Intuitively, if there is no noise or the Markov chain is not geometrically ergodic, constructing a probability distribution is impossible, which results in learning divergence. In Section VII, particularly in Tables I and II, we present numerical results concerning the empirical estimator $\hat{\phi}_T$. These findings imply that the empirical estimator's convergence might be faster than the theoretical convergence rates discussed in Theorem 4.

Remark 4: The convergence rate of the error functional, as delineated in Theorem 2, aligns with those reported in [18] and [19]. However, Theorem 4 demonstrates a slower convergence rate. To address the curse of dimensionality, we employ coupling functions. While this method allows us to reduce the search space to only 1-D function, we only have access to evaluate the summation of interaction forces among agents, represented as $\sum_{i=1}^n k_{ij}\phi(r^{ij})$, rather than directly measuring $\phi(r)$. The rate of convergence in our case is suboptimal compared to the single agent scenario [18], [19] where they permit direct measurement of the candidate and original functions. While the difference in measurement can partially explain the slower convergence rate in the proposed method, one may achieve an optimal rate by employing a tighter concentration inequality.

However, our approach, despite its slower sampling rate, has the advantage of being unaffected by the number of agents, in contrast to other frameworks where the sample complexity typically scales with $\tilde{O}((nd)^2)$. This aspect significantly lowers the overall sample complexity and helps mitigate the curse of dimensionality in large networks. Notably, in general, nonlinear setups, such as those in [19], the convergence rate is heavily dependent on the number of agents. Our framework addresses these limitations, offering a tradeoff that facilitates learning in large-scale systems, even with a slower rate per trajectory. In summary, while our approach exhibits a slower per-trajectory rate due to its specialized structure and requirements, it benefits from being unaffected by network size. As a result, the single sample trajectory approach we present improves the overall complexity and computational cost, achieving the same learning accuracy with greater efficiency.

The primary rationale for employing a weighted measure for the coupling function ϕ in Theorem 4, as opposed to the

TABLE I

ERROR FUNCTIONAL, $\mathcal{E}(\hat{\phi}_T)$, THE DISTANCE OF EMPIRICAL ESTIMATOR AND THE ORIGINAL FUNCTION, $\|\phi-\hat{\phi}\|_{L^{2,*}_{\rho_T}}$, AND THE KULLBACK–LEIBLER DIVERGENCE, $D_{\mathrm{KL}}(\rho\|\hat{\rho})$, WITH DIFFERENT TRAJECTORY LENGTH T FOR THE FIRST EXAMPLE IN SECTION VII-A

T	$\mathcal{E}_T(\hat{\phi}_T)$	$\|\phi-\hat{\phi}_T\|_{L^{2,*}_\rho}$	$D_{KL}(\rho\|\hat{\rho}_T)$
10^2	0.0809	0.0917	0.0013
10^3	0.0256	0.0298	7.54×10^{-5}
10^4	0.0081	0.0117	5.63×10^{-5}
10^5	0.0026	0.0073	4.46×10^{-5}
10^6	0.0008	0.0021	2.97×10^{-5}
∞	0.0004	0.0018	2.47×10^{-5}

TABLE II

ERROR FUNCTIONAL $\mathcal{E}(\hat{\phi}_T)$ AND THE DISTANCE OF EMPIRICAL ESTIMATOR AND THE ORIGINAL FUNCTION, $\|\phi-\hat{\phi}\|_{L^{2,*}_\rho}$, WITH DIFFERENT TRAJECTORY LENGTHS T FOR THE SECOND EXAMPLE IN SECTION VII-B

T	$\mathcal{E}_T(\hat{\phi}_T)$	$\|\phi-\hat{\phi}_T\|_{L^{2,*}_\rho}$
10^2	0.2580	3.8379
10^3	0.0815	0.7556
10^4	0.0259	0.5574
10^5	0.0083	0.3606
∞	0.0011	0.3060

traditional L_2 or L_∞ norms, is to more accurately quantify the similarity between the forces exerted by different coupling functions in relation to the distance r. By applying a weight to the variations in ϕ in proportion to r, this measure concentrates on discrepancies that have a significant influence on the system's dynamics. This approach avoids overemphasizing large deviations in ϕ at greater distances r, which might have minimal impact on the overall behavior.

The findings presented in Theorem 4 demonstrate that higher values of the coercivity condition correlate with enhanced sample efficiency in the learning of the coupling function. This further underscores the impact of the hypothesis space on our problem, illustrating its critical role in shaping the learning outcomes.

VI. Learning Procedure

A. Learning Algorithm

We discuss an algorithm to learn the empirical estimator. Suppose that $\{\psi_i^{\mathcal{H}}\}_{1\le q\le Q} \subset L^\infty([0,R])$ is a prespecified frame elements [31]. We form the hypothesis space by

$$\mathcal{H} = \left\{ \psi \,\middle|\, \psi = \sum_{q=1}^{Q} \varrho_q \psi_q^{\mathcal{H}} \text{ for some } \varrho_1, \dots, \varrho_Q \in \mathbb{R} \right\}. \quad (44)$$

For every $\psi \in \mathcal{H}$, one obtains

$$\{F_\psi(x_t)\}_i = -\sum_{j=1}^{n}\sum_{q=1}^{Q} k_{ij}\varrho_q \psi_q^{\mathcal{H}}(r_t^{ij})\mathrm{r}_t^{ij}. \quad (45)$$

Let us define $v_t = \frac{x_{t+1}-x_t}{h}$. Then, using (8) results in

$$\begin{aligned}\mathcal{E}_T(\psi) &= \frac{1}{TN_e}\sum_{t=1}^{T}\|v_t - F_\psi(x_t)\|^2 \\ &= \frac{1}{TN_e}\sum_{t=1}^{T}\sum_{i=1}^{n}\left\| v_t^i + \sum_{j=1}^{n}\sum_{q=1}^{Q} k_{ij}\varrho_q\psi_q^{\mathcal{H}}(r_t^{ij})\mathrm{r}_t^{ij}\right\|^2.\end{aligned}$$

This problem (9) can be cast as a least-squares problem

$$\underset{\varrho\in\mathbb{R}^Q}{\text{minimize}}\ \frac{1}{TN_e}\|A_T\varrho - b_T\|^2 \quad (46)$$

where $\varrho := [\varrho_1, \dots, \varrho_Q]^\mathsf{T}$, $b_T := [v_1; v_2; \cdots; v_T] \in \mathbb{R}^{ndT}$, $A_T = [\bar{A}_1^\mathsf{T}, \bar{A}_2^\mathsf{T}, \dots, \bar{A}_T^\mathsf{T}]^\mathsf{T} \in \mathbb{R}^{ndT\times Q}$, and $\bar{A}_t \in \mathbb{R}^{nd\times Q}$ is given by

$$\{\bar{A}_t\}_{i,q} = -\sum_{j=1}^{n} k_{ij}\psi_q^{\mathcal{H}}\left(r_t^{ij}\right)\mathrm{r}_t^{ij}$$

for all $1 \le q \le Q$ and $1 \le i \le n$. One can write the optimal solution of (46) in a closed from

$$\hat{\varrho}_T = \left(A_T^\mathsf{T}A_T\right)^{-1}A_T^\mathsf{T}b_T \quad (47)$$

which gives us the empirical estimator

$$\hat{\phi}_T(r) = \sum_{q=1}^{Q}\hat{\varrho}_{T,q}\psi_q^{\mathcal{H}}(r). \quad (48)$$

B. Explicit Form of Coercivity Constant

We obtain an explicit form for the coercivity condition when the hypothesis space $\mathcal{H}$ is (44). When there is no prior knowledge about the coupling function, one needs to derive the probability density function ρ empirically. We recall that the coercivity constant is defined by (37). Knowing that a candidate coupling function can be represented as $\psi = \sum_{q=1}^{Q}\varrho_q\psi_q^{\mathcal{H}}\Phi_0$, it follows that:

$$\begin{aligned}\mathbb{E}_\pi\left\|F_\psi(x)\right\|^2 &= \mathbb{E}_\pi\left[\sum_{i=1}^{n}\left\|\sum_{j=1}^{n}k_{ij}\psi(r^{ij})\mathrm{r}^{ij}\right\|^2\right] \\ &= \mathbb{E}_\pi\left[\sum_{i=1}^{n}\left\|\sum_{j=1}^{n}\sum_{q=1}^{Q}k_{ij}\varrho_q\psi_q^{\mathcal{H}}(r^{ij})\mathrm{r}^{ij}\right\|^2\right] \\ &= \mathbb{E}_\pi\left[\sum_{i=1}^{n}\varrho^\mathsf{T}\Upsilon_i^{\mathcal{H}}\varrho\right] = \varrho^\mathsf{T}\Upsilon_{\mathcal{H}}\varrho\end{aligned}$$

where $\Upsilon_{\mathcal{H}} \in \mathbb{R}^{Q\times Q}$ is a positive semidefinite matrix defined by

$$\Upsilon_{\mathcal{H}} = \mathbb{E}_\pi\left[\sum_{i=1}^{n}\Upsilon_i^{\mathcal{H}}\right]$$

and the elements of $\Upsilon_i^{\mathcal{H}} \in \mathbb{R}^{Q\times Q}$ are

$$\left(\Upsilon_i^{\mathcal{H}}\right)_{qq'} = \left(\sum_{j=1}^{n}k_{ij}\psi_q^{\mathcal{H}}(r^{ij})\mathrm{r}^{ij}\right)^\mathsf{T}\left(\sum_{j'=1}^{n}k_{ij'}\psi_{q'}^{\mathcal{H}}(r^{ij'})\mathrm{r}^{ij'}\right).$$

Similarly, one can evaluate the denominator term in (37) and obtain

$$\begin{aligned}\|\psi\|_{L_\rho^{2,*}}^2 &= \int_0^R(\psi(r)r)^2\rho(dr) \\ &= \int_0^R\left(\sum_{q=1}^{Q}\varrho_q\psi_q^{\mathcal{H}}(r)r\right)^2\rho(dr) = \varrho^\mathsf{T}\Xi_{\mathcal{H}}^\mathsf{T}\varrho\end{aligned}$$

in which $\Xi_{\mathcal{H}}^\mathsf{T} \in \mathbb{R}^{Q\times Q}$ is given by

$$\left(\Xi_{\mathcal{H}}\right)_{qq'} = \int_0^R \psi_{q'}^{\mathcal{H}}(r)\psi_q^{\mathcal{H}}(r)r^2\rho(dr)$$

for all $q, q' \in \{1, 2, \dots, Q\}$. By definition, $\Xi_{\mathcal{H}}$ is a positive semidefinite matrix. Assume that ϱ_* is an eigenvector of $\Xi_{\mathcal{H}}$ that corresponds to a zero eigenvalue. From (24), one has

$$\varrho_*^\mathsf{T}\Xi_{\mathcal{H}}\varrho_* = \int_0^R\left(\psi_*(r)r\right)^2\rho(dr) = 0 \quad (49)$$

where $\psi_* = \sum_{q=1}^{Q}\varrho_{*,q}\psi_q^{\mathcal{H}}$. Equation (49) shows that ψ_* is either zero or orthogonal to the probability measure ρ. In other words, the subset of the hypothesis space $\mathcal{H}$ that is orthogonal to ρ, which are not informative for learning purposes, is the null space of $\Xi_{\mathcal{H}}$; hence, we shall exclude them from learning. From the above derivation, one can conclude that

$$c_{\mathcal{H}} = \inf_{\varrho\notin\ker(\Xi_{\mathcal{H}})}\frac{\varrho^\mathsf{T}\Upsilon_{\mathcal{H}}\varrho}{\varrho^\mathsf{T}\Xi_{\mathcal{H}}\varrho} \quad (50)$$

where $\ker(\Xi_{\mathcal{H}})$ is the null-space of $\Xi_{\mathcal{H}}$, which is minimizing the generalized Rayleigh quotient. Suppose that $\Xi_{\mathcal{H}}^{\frac{1}{2}}$ is the Cholesky decomposition of $\Xi_{\mathcal{H}}$, i.e., $\Xi_{\mathcal{H}} = \Xi_{\mathcal{H}}^{\frac{1}{2}} \Xi_{\mathcal{H}}^{\frac{1}{2}\mathsf{T}}$. Then, the coercivity constant can be obtained through

$$c_{\mathcal{H}} = \lambda_{\min}\left(\left(\Xi_{\mathcal{H}}^{\frac{1}{2}}\right)^{-1} \Upsilon_{\mathcal{H}} \left(\Xi_{\mathcal{H}}^{\frac{1}{2}}\right)^{-\mathsf{T}}\right). \tag{51}$$

The hypothesis space $\mathcal{H}$ will not be coercive if $\Upsilon_{\mathcal{H}}$ has zero eigenvalues where their corresponding eigenvectors do not belong to $\ker(\Xi_{\mathcal{H}})$.

The computation of matrices $\Upsilon_{\mathcal{H}}$ and $\Xi_{\mathcal{H}}$ requires a complete knowledge of the probability distribution ρ. Since the agent distances are known from the samples, one can empirically approximate $\Upsilon_{\mathcal{H}}$ and $\Xi_{\mathcal{H}}$, even though the probability distribution ρ is unknown.

VII. Simulation Results

To validate our theoretical results, we provide numerical studies for two different classes of dynamical networks, namely, the first-order version of Cucker–Smale's [4] consensus network model and a first-order dynamical network inspired by the formation control problem, in which agents start from a random initial condition and attempt to maintain a specific distance from their nearby neighbors.

Metric (24) measures the distance between a given function and the original coupling function. This measure requires integration over the interval $[0,\ R]$, which makes the pointwise comparison between the two functions implausible. The square of the pointwise differences of the two functions, i.e., $(\psi(r) - \phi(r))^2$, does not consider the fact that convergence is subject to the probability distribution ρ. To remedy this issue, we define

$$\nu_{\rho,\psi}(r) \ = \ |\left(\phi(r) - \psi(r)\right) r|^2 \rho(r) \tag{52}$$

which measures the distance between the candidate coupling function and the original coupling function at every $r \in [0,\ R]$ weighted by probability density $\rho(r)$. In several applications, e.g., risk analysis and prediction, it is crucial to find a coupling function that can recreate the stochastic characteristics of the original system. To this end, we define the probability distribution $\hat{\rho}_T$ by replacing ϕ in (1) with $\hat{\phi}_T$, i.e., the stationary probability distribution of the distances between the agents in swarm dynamics

$$\hat{x}_{t+1}^i = \hat{x}_t^i + h\sum_{j=1}^{n} k_{ij}\hat{\phi}_T\left(\|\hat{x}_t^j - \hat{x}_t^i\|\right)\left(\hat{x}_t^j - \hat{x}_t^i\right) + hw_t^i.$$

To compare the two probabilities, we employ the Kullback–Leibler divergence measure

$$D_{\mathrm{KL}}\left(\rho \| \hat{\rho}_T\right) = \int_0^R \rho(r) \log\left(\frac{\rho}{\hat{\rho}_T}\right) dr$$

to quantify how far these two probability distributions are from each other.

A. Cucker–Smale Model

In Example 2, we discussed this class of first-order dynamical networks, where they can be characterized using the following spatially decaying coupling functions [32]:

$$\phi(r) = \Gamma\left(1 + r^2\right)^{-\eta} \tag{53}$$

where parameters $\Gamma, \eta > 0$ determine coupling strength between the agents. The state space of each agent is $\mathbb{R}^2$, and each agent is driven by a uniform bounded noise with mean zero and $\mathbb{E}[w_i^{\mathsf{T}} w_i] = (\omega^2/3)I$. It is assumed that there is no prior knowledge about the coupling function. Thus, the class of simple functions is used as the hypothesis space, i.e., every function $\psi \in \mathcal{H}$ can be represented as

$$\psi(r) = \sum_{q=1}^{Q} \varrho_q \mathbf{1}_q(r)$$

where the indicator function $\mathbf{1}_q : \mathbb{R} \to \{0, 1\}$ is defined by

$$\mathbf{1}_q(r) = \begin{cases} 1 & \text{if } r \in [R\frac{q-1}{Q},\ R\frac{q}{Q}) \\ 0 & \text{if } r \notin [R\frac{q-1}{Q},\ R\frac{q}{Q}) \end{cases}$$

$R = 0.6$ given by (16). It is assumed that the initial condition of every agent is zero and that they are all-to-all connected with network parameters $\Gamma = 1, \eta = 0.4$, and $Q = 20$, and noise amplitude $\omega = 10$. We assume that the network is symmetric, and therefore, all communications have the same weights, i.e., $k_{ij} = 1$, for all $i \neq j$. From our discussion in Example 1 and the fact that graph $\mathcal{G}$ is complete, it follows that if $h < \frac{1}{S_0 n}$, then the network dynamics (1) is ergodic. For the guaranteed ergodicity of network with 25 agents, the above inequality transforms to $h < 0.04$. Therefore, we chose $h = 0.01$ to make sure that the sampling time h is sufficiently small to ensure the required ergodicity property of the dynamical network.

Fig. 2 shows the empirical estimator $\hat{\phi}_T$, the empirical probability distribution ρ_T, and the pointwise distance between $\hat{\phi}_T$ and ϕ for different sample trajectory lengths $T = \{10^3,\ 10^4,\ 10^5\}$. The empirical estimation of the coupling function, i.e., $\hat{\phi}_T$, converges pointwise to the original function, as illustrated in Fig. 2, in the regions where the probability measure ρ is nonzero. The learning algorithm is anticipated to converge more accurately at the probability distribution's peaks, as these points are where the agent's distance information is found in abundance.

The hypothesis space $\mathcal{H}$ is constructed by the indicator functions that are orthogonal to each other, i.e.,

$$\int_0^R \psi_q(r)\psi_{q'}(r) r^2 \rho(dr) = 0$$

for all $q \neq q'$. Therefore, Ξ_M is a diagonal matrix. We can further simplify (51) and get $c_{\mathcal{H}} = \lambda_{\min}(\Xi_{\mathcal{H}}^{-1}\Upsilon_{\mathcal{H}}) = 3.8469 > 0$, which indicates that the candidate hypothesis space is coercive and convex. Thus, Theorem 3 can be applied, which asserts that the empirical estimator converges to the original function with respect to $L_\rho^{2,*}$-norm, i.e., the convergence depends on the probability density ρ, and it is not pointwise. From Fig. 2, one

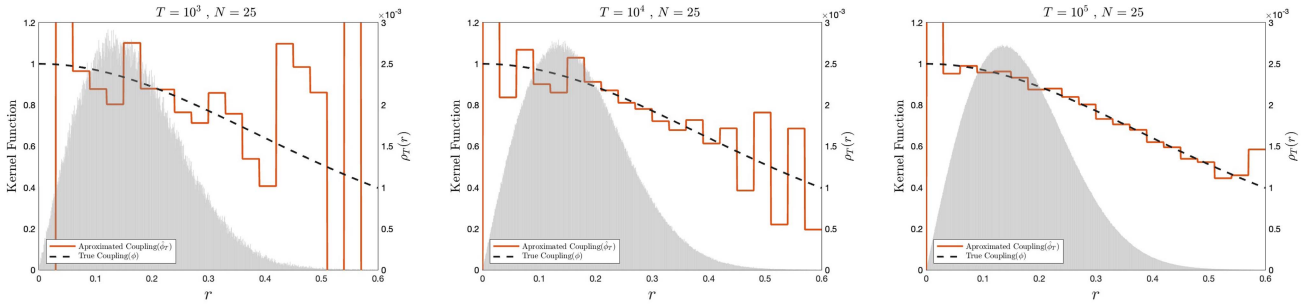

Fig. 2. *True* coupling function ϕ, *approximated* couplings $\hat{\phi}_T$ and *initial* function guess ϕ_0, and *probability density* function ρ_T for different trajectory length T discussed in the first example in Section VII-A.

can conclude that $(\hat{\phi}_T - \phi)^2$ can assume relatively large values compared to $\nu_{\rho,\hat{\phi}_T(r)}$, while their peaks are in different regions.

Table I displays the empirical error $\mathcal{E}_T(\hat{\phi}_T)$, the distance of the estimated and the original couplings $\|\phi - \hat{\phi}_T\|_{L^{2,*}_\rho}$, and the Kullback–Leibler divergence $D_{\mathrm{KL}}(\rho\|\hat{\rho})$ for various trajectory lengths. We remark that the $D_{\mathrm{KL}}(\rho\|\hat{\rho}_T)$ is computed empirically from the sample trajectory. The results in Table I are in line with Theorem 3, where both the empirical error and the distance between the estimator and the original function are expected to decrease to certain saturation values as T increases.

It should be emphasized that the original coupling function does not belong to the hypothesis space. As a result, the error function $\mathcal{E}_T(\hat{\phi}_T)$ is expected to reach a saturation level. On the other hand, the Kullback–Leibler divergence $D_{\mathrm{KL}}(\rho\|\hat{\rho}_T)$ decreases at a slower rate than the empirical error. This hints that even with small sample trajectories, which result in an estimator that is usually far from the original function, the probability distribution $\hat{\rho}_T$ can be close to ρ as the network structure remains intact.

B. Collision Avoidance Formation

We consider the formation control of a group of agents along the horizontal axis that is coupled through a graph with chain topology [33]. This model appears in several applications, including the placement of mobile sensors and surveillance with flying machines such as satellites. To avoid collision between every two consecutive agents, we use a nonlinear coupling that generates repulsive force when the agents are too close to each other and attractive force when they are far away. The control objective is to maintain these agents at a certain distance r_0 from each other in the presence of exogenous noise. The underlying communication graph $\mathcal{G}_0$ is an undirected chain graph in which the agents are only allowed to communicate with their nearest neighbors. The dynamics of the network is given by (1) with $d = 1$, and $k_{ij} = 1$ if $j \in \{i+1, i-1\}$ and zero, otherwise. The coupling function

$$\phi(r) = \frac{\Gamma(r - r_0)^2}{(a - (r - r_0)^3)^\eta} \tag{54}$$

where a, Γ, and η are positive constants. Fig. 4 depicts the coupling function, and it is assumed that each agent is disturbed by a uniform bounded noise with mean zero and $\mathbb{E}[w_i w_i^{\mathsf{T}}] = (\omega^2/3)I$. In order to achieve the desired formation, we change the equilibrium of the swarm dynamics (1) to $\mathbf{b} = [0,\, r_0,\, 2r_0, \ldots, nr_0]$. It is assumed that there is no prior knowledge about the coupling function and that the hypothesis space is the set of all polynomials with order less than or equal to $Q = 10$, i.e., every function $\psi \in \mathcal{H}$ can be represented by

$$\psi(r) = \sum_{q=1}^{Q} \varrho_q r^q. \tag{55}$$

Adopting polynomials as our hypothesis space will allow us to apply the method introduced in Section VI-B to estimate the coercivity condition. After calculations, the coercivity is $c_{\mathcal{H}} = 0.0371$, which shows that the candidate hypothesis space is coercive with respect to probability distribution ρ. In this case study, the number of agents is $n = 20$, the coupling parameters are $\Gamma = 10$, $\eta = 0.4$, $r_0 = 1$, and $a = 1.01$, and the initial conditions are drawn randomly from the uniform distribution over $[-20, 20]$. It is further assumed that the maximum communication range between the agents is 3 units, i.e., $R_0 = 3$; as a result, the parameter $S_0 = 43.0957$. Example 1 states that in order for the current path networks to have counteractive dynamics, the time step h needs to satisfy $h \leq 0.0118$; therefore, we chose $h = 0.01$. As a consequence of Theorem 1, the dynamical network with the proposed coupling function is geometrically ergodic. The numerical results for different trajectory length $T = \{10^2, 10^3, 10^4, 10^5\}$ are depicted in Fig. 3. The top row shows the probability distribution ρ_T, along with the original coupling function ϕ and the learned coupling function ϕ_T. The second row shows the distance between the original and the learned coupling functions with respect to the weighted pointwise error (52). The last row illustrates the pointwise squared error between the original and the learned coupling functions. For better illustration, the last two rows have different scales as the error levels change drastically with the length of the sample trajectory.

Fig. 3 illustrates that the learning accuracy and the distribution function ρ_T depend on the length of the sampling trajectory. As $T \to \infty$, the probability ρ_T converges to the stationary probability ρ. The candidate hypothesis space for this experiment is coercive. Thus, Theorem 3 can be applied, which implies that the convergence happens with respect to $L^{2,*}_\rho$-norm. Despite the fact that the estimation diverges from the original couplings

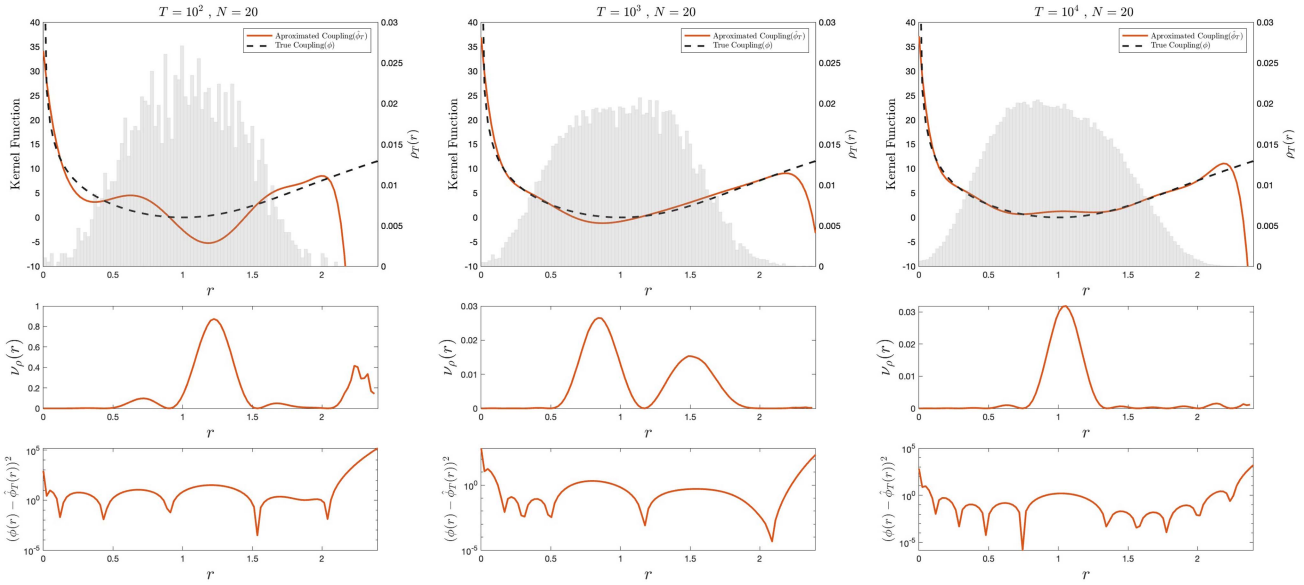

Fig. 3. *True* coupling function ϕ, *approximated* couplings $\hat{\phi}_T$ and *initial* function guess ϕ_0, *probability density* function ρ_T, the *pointwise* distance of estimated function and original kernel, $\nu_{\rho,\hat{\phi}_T}(r)$, and the squared error $(\phi - \hat{\phi}_T)^2$, with different trajectory length T for the case study in Section VII-B.

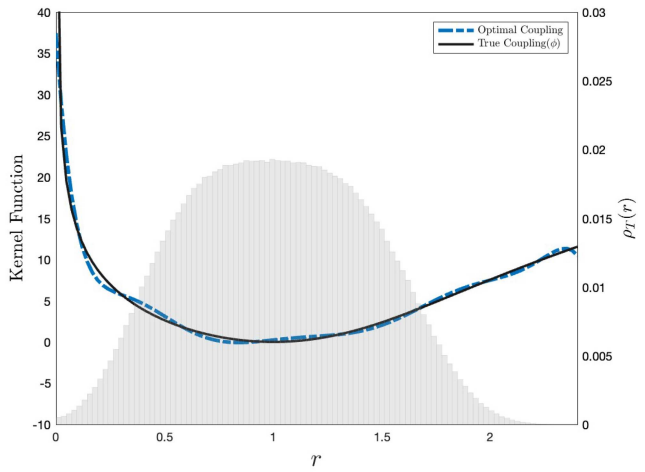

Fig. 4. *Original* coupling function ϕ, probability *density* ρ, and the *best approximation* of original couplings, ϕ, over hypothesis space $\mathcal{H}$ for the second example in Section VII-B.

in some regions, one can observe that $\nu_\rho(r)$ converges to zero almost everywhere on the interval $[0,\ R]$. Hence, the estimator converges over those regions where information are found in abundance.

The numerical values of the learning error $\mathcal{E}_T(\hat{\phi}_T)$ and the distance of the estimated and the original function $\|\phi - \hat{\phi}_T\|_{L^{2,*}_\rho}$ are reported in Table II. Despite the fact that both empirical error $\mathcal{E}_T$ and the distance between the empirical estimator and the original coupling function are strictly decreasing as sample trajectory length increases, they both reach a saturation level. However, the reason why these parameters saturate is different in each case. According to (26), $\mathcal{E}_T(\psi)$ contains two parts, where the first term depends on the difference between the candidate coupling function and the original one, while the second term, which is given by σ^2/N_e, depends solely on the noise variance. On the contrary, the source of saturation in $\|\phi - \hat{\phi}_T\|_{L^{2,*}_{\rho_T}}$ originates from the limitation of the hypothesis space $\mathcal{H}$ to approximate the original coupling function, which is discussed in Theorem 3. The distance between the empirical estimator from the original coupling function tends to be the distance between the original coupling function and $\mathcal{H}$ as the original coupling function does not belong to $\mathcal{H}$. Fig. 4 illustrates the best coupling function that one can learn from $\mathcal{H}$ alongside the expected probability density ρ. This function is obtained by taking samples from ϕ with respect to the probability density function ρ. It can be seen that $\hat{\phi}_T$ is close to the best possible approximation.

VIII. Conclusion

We develop a method for learning nonlinear coupling functions in stochastic dynamical networks, requiring only a single, extended sample trajectory. This involves proving that these networks yield geometrically ergodic trajectories, meaning new samples along the trajectory are informative for learning. We quantify various error bounds for learning precision and show that as the trajectory length increases, the learning quality gradually nears its optimal level.

References

[1] M. Kurt, A. Mivehchi, and K. Moored, "High-efficiency can be achieved for non-uniformly flexible pitching hydrofoils via tailored collective interactions," *Fluids*, vol. 6, no. 7, 2021, Art. no. 233.

[2] E. Rimon and D. Koditschek, "Exact robot navigation using artificial potential functions," *IEEE Trans. Robot. Automat.*, vol. 8, no. 5, pp. 501–518, Oct. 1992.

[3] T. Vicsek, A. Czirók, E. Ben-Jacob, I. Cohen, and O. Shochet, "Novel type of phase transition in a system of self-driven particles," *Phys. Rev. Lett.*, vol. 75, no. 6, 1995, Art. no. 1226.

[4] F. Cucker and S. Smale, "Emergent behavior in flocks," *IEEE Trans. Autom. Control*, vol. 52, no. 5, pp. 852–862, May 2007.
[5] F. Cucker and S. Smale, "On the mathematics of emergence," *Japanese J. Math.*, vol. 2, no. 1, pp. 197–227, 2007.
[6] S. H. Strogatz, "Norbert wiener's brain waves," in *Frontiers in Mathematical Biology*, Berlin, Germany: Springer, 1994, pp. 122–138.
[7] M. Mohri, A. Rostamizadeh, and A. Talwalkar, *Foundations of Machine Learning*. Cambridge, MA, USA: MIT Press, 2018.
[8] F. Cucker and D. X. Zhou, *Learning Theory: An Approximation Theory Viewpoint*, vol. 24. Cambridge, U.K.: Cambridge Univ. Press, 2007.
[9] T. Poggio and C. R. Shelton, "On the mathematical foundations of learning," *Amer. Math. Soc.*, vol. 39, no. 1, pp. 1–49, 2002.
[10] M. Hardt, T. Ma, and B. Recht, "Gradient descent learns linear dynamical systems," *J. Mach. Learn. Res.*, vol. 19, no. 29, pp. 1–44, 2018.
[11] H. Moritz, T. Ma, and B. Recht., "Gradient descent learns linear dynamical systems," *J. Mach. Learn. Res.*,, vol. 19.29, pp. 1–44, 2018.
[12] S. L. Brunton, J. L. Proctor, and J. N. Kutz, "Discovering governing equations from data by sparse identification of nonlinear dynamical systems," *Proc. Nat. Acad. Sci. USA*, vol. 113, no. 15, pp. 3932–3937, 2016.
[13] S. Dean, S. Tu, N. Matni, and B. Recht, "Safely learning to control the constrained linear quadratic regulator," in *2019 Amer. Control Conf.*, 2019, pp. 5582–5588.
[14] M. Bongini, M. Fornasier, M. Hansen, and M. Maggioni, "Inferring interaction rules from observations of evolutive systems I: The variational approach," *Math. Models Methods Appl. Sci.*, vol. 27, no. 05, pp. 909–951, 2017.
[15] F. Lu, M. Zhong, S. Tang, and M. Maggioni, "Nonparametric inference of interaction laws in systems of agents from trajectory data," *Proc. Nat. Acad. Sci. USA*, vol. 116, no. 29, pp. 14424–14433, 2019.
[16] F. Lu, M. Maggioni, and S. Tang, "Learning interaction kernels in heterogeneous systems of agents from multiple trajectories," *J. Mach. Learn. Res.*, vol. 22, pp. 1–67, 2021.
[17] X. Chen, "Maximum likelihood estimation of potential energy in interacting particle systems from single-trajectory data," *Electron. Commun. Probability*, vol. 26, 2021, Art. no. 45.
[18] D. Foster, T. Sarkar, and A. Rakhlin, "Learning nonlinear dynamical systems from a single trajectory," in *Proc. Conf. Learn. Dyn. Control*, 2020, pp. 851–861.
[19] I. Ziemann and S. Tu, "Learning with little mixing," in *Proc. 36th Int. Conf. Neural Inf. Process. Syst.*, 2022, pp. 4626–4637.
[20] I. M. Ziemann, H. Sandberg, and N. Matni, "Single trajectory nonparametric learning of nonlinear dynamics," in *Proc. Conf. Learn. Theory*, PMLR, 2022, pp. 3333–3364.
[21] Y. Sattar and S. Oymak, "Non-asymptotic and accurate learning of nonlinear dynamical systems," *J. Mach. Learn. Res.*, vol. 23, no. 1, pp. 6248–6296, 2022.
[22] Y. Sattar, S. Oymak, and N. Ozay, "Finite sample identification of bilinear dynamical systems," in *Proc. IEEE Conf. Decis. Control (CDC)*, 2022, pp. 6705–6711.
[23] D. B. Cline and H.-M. H. Pu, "Geometric ergodicity of nonlinear time series," *Statistica Sinica*, vol. 9, pp. 1103–1118, 1999.
[24] H. Tong, *Non-Linear Time Series: A Dynamical System Approach*. Oxford, U.K.: Oxford Univ. Press, 1990.
[25] C. W. Gardiner et al., *Handbook of Stochastic Methods*. Berlin, Germany: Springer, 1985.
[26] S. T. Jensen and A. Rahbek, "On the law of large numbers for (geometrically) ergodic Markov chains," *Econometric Theory*, vol. 23, no. 4, pp. 761–766, 2007.
[27] S. P. Meyn and R. L. Tweedie, *Markov Chains and Stochastic Stability*. Berlin, Germany: Springer, 2012.
[28] D. Kristensen, "Geometric ergodicity of a class of Markov chains with applications to time series models," Available at SSRN 831068, Oct. 19, 2005.
[29] G. O. Roberts and J. S. Rosenthal, "Variance bounding Markov chains," *Ann. Appl. Prob.*, vol. 18, no. 3, pp. 1201–1214, 2008.
[30] O. Haggstrom and J. Rosenthal, "On variance conditions for Markov chain CLTs," *Electron. Commun. Probab.*, vol. 12, pp. 454–464, 2007.
[31] O. Christensen et al., *An Introduction to Frames and Riesz Bases*. Berlin, Germany: Springer, 2003.
[32] F. Cucker and E. Mordecki, "Flocking in noisy environments," *J. de Mathématiques Pures et Appliquées*, vol. 89, no. 3, pp. 278–296, 2008.
[33] G. Liu, C. Somarakis, and N. Motee, "Risk of cascading failures in time-delayed vehicle platooning," in *Proc. IEEE Conf. Decis. Control*, 2021, pp. 4841–4846.

Arash Amini received the B.Sc. degree in mechanical engineering from the Sharif University of Technology, Tehran, Iran, in 2017, and the M.Sc. and Ph.D. degrees in mechanical engineering from Lehigh University, Bethlehem, PA, USA, in 2022 and 2023, respectively.

Since 2023, he has been a Postdoctoral Associate with the Oden Institute of Computational Science, University of Texas at Austin, Austin, TX, USA. His research interests include autonomy and information flow in large networks.

Qiyu Sun received the Ph.D. degree in mathematics from Hangzhou University, Hangzhou, China, in 1990.

He is currently a Professor of mathematics with the University of Central Florida, Orlando, FL, USA. He has authored or coauthored more than 100 papers and written a book *An Introduction to Multiband Wavelets* with N. Bi and D. Huang. His research interests include applied and computational harmonic analysis, sampling theory, phase retrieval, and graph signal processing.

Nader Motee (Senior Member, IEEE) received the B.Sc. degree in electrical engineering from the Sharif University of Technology, Tehran, Iran, in 2000, and the M.Sc. and Ph.D. degrees in electrical and systems engineering from University of Pennsylvania, Philadelphia, PA, USA, in 2006 and 2007, respectively.

He is currently a Professor with Lehigh University, Philadelphia, PA.

Dr. Motee was the recipient of several awards, including the 2008 AACC Hugo Schuck Best Paper Award, the 2013 AFOSR YIP, the 2015 NSF CAREER, and the 2016 ONR YIP.